

Proceedings of the Institution of
Civil Engineers
Structures & Buildings 161
February 2008 Issue SBI
Pages 29–39
doi: 10.1680/stbu.2008.161.1.29

Paper 700016
Received 28/04/2007
Accepted 13/11/2007

Keywords: beams & girders/
concrete structures



Keun-Hyeok Yang
Assistant Professor,
Department of Architectural
Engineering, Mokpo National
University, South Korea



Ashraf F. Ashour
Senior Lecturer, University
of Bradford, UK



Jin-Kyu Song
Associate Professor,
Chonnam National
University, South Korea



Eun-Taik Lee
Associate Professor,
Chungang University, South
Korea

ice
Institution of Civil Engineers

Neural network modelling of RC deep beam shear strength

K.-H. Yang MSc Archi. Engng, PhD, PE, A. F. Ashour MSc, PhD, CEng, MStructE, J.-K. Song MSc, PhD, Archi. Engng and E.-T. Lee MSc, PhD, Archi. Engng.

A $9 \times 18 \times 1$ feed-forward neural network (NN) model trained using a resilient back-propagation algorithm and early stopping technique is constructed to predict the shear strength of deep reinforced concrete beams. The input layer covering geometrical and material properties of deep beams has nine neurons, and the corresponding output is the shear strength. Training, validation and testing of the developed neural network have been achieved using a comprehensive database compiled from 362 simple and 71 continuous deep beam specimens. The shear strength predictions of deep beams obtained from the developed NN are in better agreement with test results than those determined from strut-and-tie models. The mean and standard deviation of the ratio between predicted capacities using the NN and measured shear capacities are 1.028 and 0.154, respectively, for simple deep beams, and 1.0 and 0.122, respectively, for continuous deep beams. In addition, the trends ascertained from parametric study using the developed NN have a consistent agreement with those observed in other experimental and analytical investigations.

NOTATION

A_c	beam section area
A_h	area of horizontal web reinforcement
A_s	area of longitudinal bottom reinforcement
A'_s	area of longitudinal top reinforcement
A_{str}	section area of concrete strut
A_v	area of vertical web reinforcement
A_{wj}	area of the j th layer of reinforcement crossing a strut
a	shear span
b_w	width of beam section
c	cover of longitudinal bottom reinforcement
c'	cover of longitudinal top reinforcement
d	effective depth of beam section
d_s	diameter of longitudinal reinforcement
d_w	distance from top surface of beam to intersection of web reinforcement with the centreline of strut
f'_c	concrete compressive strength
f_y	yield strength of longitudinal bottom reinforcement
f'_y	yield strength of longitudinal top reinforcement
f_{yh}	yield strength of horizontal web reinforcement
f_{yv}	yield strength of vertical web reinforcement
f_{yw}	yield strength of web reinforcement crossing a strut

h	overall depth of beam section
jd	distance between the centre of top and bottom nodes
l_o	maximum spacing of web reinforcement for beams with web reinforcement and strut length for beams without web reinforcement
l_p	width of loading or support plate
l_s	strut length
N	total number of training subset
n	modular ratio of steel reinforcement to concrete
p_i	original values of data set
$(p_i)_n$	normalised values of data set
$(p_i)_{max}$	maximum value of the parameter under normalisation
$(p_i)_{min}$	minimum value of the parameter under normalisation
s_h	spacing of horizontal web reinforcement
s_v	spacing of vertical web reinforcement
s_{wj}	spacing of the j th layer of reinforcement crossing a strut
T_i	target output of the data i
V_n	shear strength
w_s	width of concrete strut
w_t	depth of bottom node
w'_t	depth of top node
β	the ratio of the end support reaction to the applied load in continuous deep beams
γ_{cs}	ratio of predicted and measured shear capacities
$\gamma_{cs,m}$	average of γ_{cs}
$\gamma_{cs,s}$	standard deviation of γ_{cs}
$(\theta_r)_j$	angle between reinforcing bar j and the axis of concrete strut
θ_s	angle between concrete strut and longitudinal axis of beam
θ_w	angle of web reinforcement to longitudinal axis of beam
λ_n	normalised shear strength $\left(\frac{V_n}{b_w h \sqrt{f'_c}}\right)$
ν_e	effectiveness factor of concrete
ρ_h	horizontal web reinforcement ratio $\left(\frac{A_h}{b_w s_h}\right)$
ρ_s	longitudinal bottom reinforcement ratio $\left(\frac{A_s}{b_w d}\right)$
ρ'_s	longitudinal top reinforcement ratio $\left(\frac{A'_s}{b_w d}\right)$
ρ_v	vertical web reinforcement ratio $\left(\frac{A_v}{b_w s_v}\right)$
ϕ_b	longitudinal bottom reinforcement index $\left(\frac{\rho_s f_y}{f'_c}\right)$
ϕ_h	horizontal web reinforcement index $\left(\frac{\rho_h f_{yh}}{f'_c}\right)$
ϕ_t	longitudinal top reinforcement index $\left(\frac{\rho'_s f'_y}{f'_c}\right)$

ϕ_v vertical web reinforcement index $\left(\frac{\rho_v f_{yv}}{f_c}\right)$

1. INTRODUCTION

Reinforced concrete deep beams, generally defined as beams having shear span-to-overall depth ratio not exceeding 2.0, are common structural members having useful applications as load distribution elements such as transfer girders, pile caps and foundation walls in tall buildings. They are classified as discontinuity regions (D-regions) having a non-linear strain distribution over the cross-section depth owing to a smaller shear span-to-overall depth ratio (≤ 2.0) and extraordinarily high concentric loads.¹ As a result, shear deformations are not negligible. In addition, the coexistence of high shear and high moment within interior shear spans of continuous deep beams leads to a significant reduction of effective strength of concrete struts directly carrying the applied loads to supports.²⁻⁴ The conventional elastic solution or shear hypotheses developed for slender beams would therefore be inadequate for the evaluation of the structural behaviour of deep beams.

Several investigations on predicting shear strength of deep beams can be classified as empirical formulae based on test results of simply supported deep beams,⁵⁻⁹ strut-and-tie models,^{1,10-13} mechanism analysis^{14,15} using upper-bound theorem of plasticity theory and non-linear finite element analyses.^{16,17} Ashour² and Rogowsky *et al.*³ showed that empirical formulae, such as ACI 318-99⁹ (unchanged since ACI 318-83) and Construction Industry Research and Information Association (CIRIA) Guide 2,⁸ failed to evaluate the shear transfer capacities of horizontal web reinforcement and concrete struts of continuous deep beams tested. The strut-and-tie model is a powerful analytical tool, which can easily represent the load-transfer mechanism of deep beams, but it is difficult to determine the real dimension of concrete struts and shear transfer mechanism of vertical and horizontal web reinforcement as pointed out by Marti.¹⁸ Mechanism analysis can provide logical shear transfer mechanism of vertical and horizontal web reinforcement, but shear transfer capacity of concrete is varied according to the effectiveness factor of concrete, which depends on the material characteristics and geometrical dimensions of concrete members.^{18,19} Non-linear finite element analyses, which are usually carried out as a complementary tool to verify experimental work, give detailed solutions. According to Wang *et al.*¹⁵ and Ashin,¹⁶ however, they require a lot of time, input parameters and calibration to be useful in practical design.

Artificial neural network (NN) techniques can be employed as a useful tool to precisely predict structural performance of concrete members if many reliable test results are provided as shown by several researches.²⁰⁻²² Goh²⁰ and Sanad and Saka²¹ showed that shear strength of deep beams can be better predicted by multi-layered feed-forward NNs than other existing formulae. It should, however, be noted that NNs are hardly capable of giving extrapolation for parameters outside the network training set as they can learn and generalise through only previous patterns.^{23,24} It is therefore important to provide NNs with more test data to find acceptable solutions to different situations.

In the present study, multi-layered feed-forward NNs trained with the back-propagation algorithm are developed to model

the non-linear relationship between shear strength of deep beams and different influencing parameters. An extensive database of simple and continuous deep beams tested by different researchers is used to train, generalise and verify the developed NN. Statistical distributions of predictions obtained from the trained NN are compared with those determined from strut-and-tie models proposed by ACI 318-05,¹ Siao¹⁰ and Tan and Cheng.¹² Also, a parametric study is carried out to ensure whether training and validation subsets in the developed NN were suitably built.

2. NEURAL NETWORK MODELLING

2.1. Network architecture for back-propagation

A typical multi-layered feed-forward NN without input delay commonly consists of input layer, one or more hidden layers and output layer as shown in Fig. 1, where p indicates the input vector, iw and lw give the weight matrices for input and hidden layers, respectively, b represents the bias vector and n is the net input passed to the transfer function f to obtain the neuron's output vector y . Input data of input layer given from outside feed into hidden layers connecting input and output layers in a forward direction, and then useful characteristics of input data are extracted and remembered in hidden layers to predict the output. Finally NN predictions are produced through the output layer. Each processing element would have many inputs, but it can send out only one output.

Among the available techniques to train a network, back-propagation is generally known to be the most powerful and widely used for NN applications.^{21,22} To obtain some desired outputs, weights, which represent connection strength between neurons, and biases are adjusted using a number of training inputs and the corresponding target values. The network error, difference between calculated and expected target patterns in a multi-layered feed-forward network, is then back propagated from the output layer to the input layer to update the network weights and biases. The adjusting process of neuron weights and biases is carried out until the network error arrives at a specific level of accuracy.

2.2. Generalisation

One of the problems that occur during NN training is the so-called overfitting²³ as the network has memorised the training features, but it has not learned to generalise new patterns. According to Shi,²⁵ training data evenly distributed over the

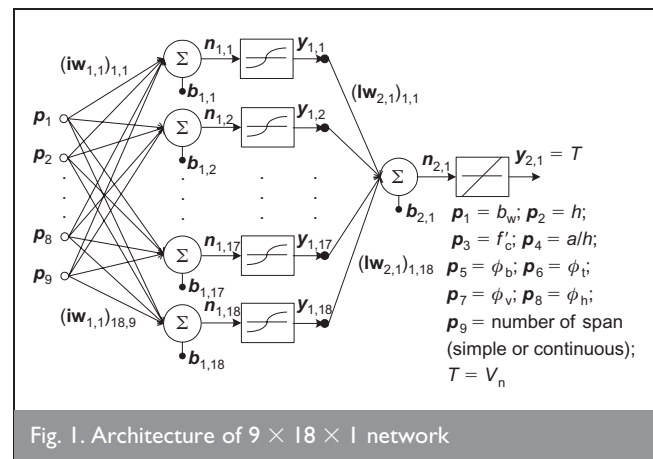


Fig. 1. Architecture of $9 \times 18 \times 1$ network

entire space enable the NN successfully to achieve the desired behaviour and the network error for new input data can be also small. One of the most effective methods to improve generalisation of NNs is early stopping.^{23,25} In this technique, the available data are divided into three subsets: training, validation and test subsets. The training set is used for computing the gradient and updating the network weights and biases to diminish the training error. When the error on the validation set, which is monitored during the training process, increases for a specified number of iterations, the training is stopped, and then the network weights and biases at the minimum validation error are returned. The test set error is not used during the training, but it is used for verification of the NNs.

2.3. Experimental database

A total of 362 simple and 71 continuous deep beam specimens failed in shear compiled from different sources in the literature is used to train and generalise the developed NNs. In the database, 74 simple^{4,26} and 44 continuous^{2,4,27} deep beams were tested by the authors and the others compiled from published literatures: de Paiva and Siess,⁵ Ramakrishna and Ananthanarayana,⁶ Kani,²⁸ Kong *et al.*,²⁹ Manuel *et al.*,³⁰ Smith and Vantsiotis,³¹ Furuuchi *et al.*,³² Hayashikawa *et al.*,³³ Walraven and Lehwalter,³⁴ Sato *et al.*,³⁵ Tan *et al.*,³⁶⁻⁴⁰ Lee and Kim,⁴¹ and Oh and Shin⁴² for simple deep beams, and Rogowsky *et al.*³ and Asin¹⁶ for continuous deep beams. Some test specimens had no web reinforcement, whereas others were reinforced with vertical and horizontal web reinforcement: the number of simple and continuous deep beams in the database is 81 and 15, respectively, for beams without web reinforcement, 104 and 26, respectively, for beams with only vertical web reinforcement, 45 and 15, respectively, for beams with only horizontal web reinforcement, and 132 and 15, respectively, for beams with orthogonal web reinforcement. Prestressing enhances the shear capacity of deep beams.⁴³ Test results on prestressed concrete beams are, however, scarce; prestressed concrete deep beams are therefore not included in the database. The database ascertained that the shear strength of deep beams was influenced by geometrical conditions such as section width, b_w , and depth, h , longitudinal top, $\rho'_s = A'_s/b_w d$, and bottom, $\rho_s = A_s/b_w d$ reinforcement ratios, vertical, $\rho_v = A_v/b_w s_v$, and horizontal $\rho_h = A_h/b_w s_h$ web reinforcement ratios, and shear span-to-overall depth ratio, a/h , and material properties such as concrete compressive strength, f'_c , and yield strength, f_y , of reinforcing bars, where A'_s and A_s are area of longitudinal top and bottom reinforcement, respectively, d is effective section depth, A_v and s_v area and spacing of vertical web reinforcement, respectively, A_h and s_h are area and spacing of horizontal web reinforcement, respectively and a is shear span for continuous deep beams, as shown in Fig. 2

The main variables above were rearranged in the database to improve efficiency of NN training. As the influence of the amount and yield strength of longitudinal and web reinforcing bars on the shear strength of deep beams depends on concrete strength,¹⁰ longitudinal top $\phi_t = \rho'_s f'_y / f'_c$ and bottom $\phi_b = \rho_s f_y / f'_c$ reinforcement indices, and vertical $\phi_v = \rho_v f_{yv} / f'_c$ and horizontal $\phi_h = \rho_h f_{yh} / f'_c$ web reinforcement indices were used as inputs in NNs, together with b_w , h , f'_c , a/h , and supporting system as shown in Table

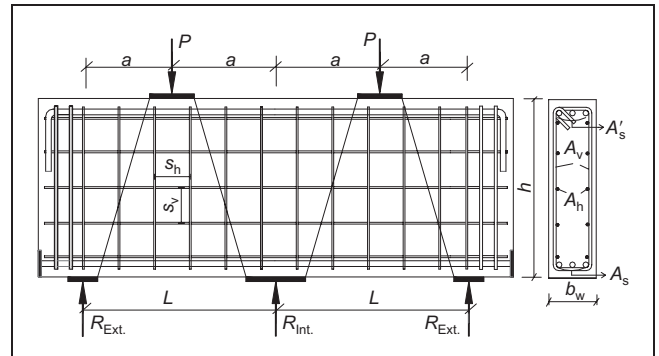


Fig. 2. Symbolic identification for deep beams in the neural network model

1, where f'_y , f_y , f_{yv} and f_{yh} represent yield strength of longitudinal top and bottom reinforcement and vertical and horizontal web reinforcement, respectively. The number of spans of deep beams (i.e. simple or continuous deep beam) was also represented in the input layer by a neuron having a numerical value of either 1 or 2 for simple and two-span deep beams, respectively. Shear strength, V_n , at failed shear span, was the only output of the NNs developed.

In the database, the shear span-to-overall depth ratio of simple and continuous deep beams ranged from 0.25 to 2.0 and from 0.5 to 2.0, respectively, the overall section depth is between 300 and 1750 mm for simple deep beams and between 400 and 1000 mm for continuous deep beams, and longitudinal bottom reinforcement index ranged between 0.04 and 0.53 for simple deep beams and between 0.05 and 0.19 for continuous deep beams. The test specimens in the database were made of concrete having a low compressive strength of 18.0 MPa and 25.0 MPa for simple and continuous deep beams, respectively, and a high compressive strength of 89.4 MPa and 68.2 MPa for simple and continuous deep beams, respectively. Test specimens having smaller concrete strength, width and depth than the lower limits stated above were excluded from the database used in the current investigation for practicality purposes.

It is recommended when using back-propagation algorithm in MATLAB version 6.0⁴⁴ that the data set is divided into three sets—training, validation and testing sets—to overcome the overfitting problem as explained above. The training data set comprises half of all data entries, and the remaining data entries are equally divided between the validation and testing sets. Little research has been conducted on the training data selection for NNs using back propagation. Jenkins^{45,46} successfully used the hypercube concept for selecting training patterns of four design parameters for reinforced concrete deep beams. It is not, however, possible to adopt this technique in the current analysis as the database was collected from different sources where intervals between discrete values are not uniform and may constitute clusters. In addition, as the number of design variables considered is nine, it would require a very high number of training data; even if only the cube corners are selected. The technique below is therefore followed to partition the database for training, validation and testing purposes. The test specimens in the database were arranged in

Input variables*		Total data		Training subset		Validation subset		Test subset	
		Min.	Max.	Min.	Max.	Min.	Max.	Min.	Max.
b_w : mm	Simple	100	300	100	300	100	300	100	300
	Continuous	120	200	120	200	120	200	120	200
h : mm	Simple	300	1750	300	1750	300	1750	300	1750
	Continuous	400	1000	400	1000	400	1000	425	1000
f'_c : MPa	Simple	18.0	89.4	18.0	89.4	18.2	82.8	18.6	79.6
	Continuous	25.0	68.2	25.0	68.2	26.5	68.2	29.4	68.2
a/h	Simple	0.25	2.0	0.25	2.0	0.25	2.0	0.25	2.0
	Continuous	0.5	2.0	0.5	2.0	0.5	2.0	0.5	2.0
ϕ_b	Simple	0.04	0.53	0.04	0.53	0.05	0.495	0.073	0.497
	Continuous	0.05	0.19	0.05	0.19	0.061	0.175	0.05	0.19
ϕ_t	Simple	—	—	—	—	—	—	—	—
	Continuous	0.05	0.19	0.05	0.19	0.054	0.175	0.054	0.19
ϕ_v	Simple	0.0	0.298	0.0	0.298	0.0	0.275	0.0	0.284
	Continuous	0.0	0.1	0.0	0.1	0.0	0.08	0.0	0.075
ϕ_h	Simple	0.0	1.836	0.0	1.836	0.0	1.763	0.0	1.49
	Continuous	0.0	0.118	0.0	0.118	0.0	0.089	0.0	0.09

Note: *Simple and continuous deep beams were identified in the input layer as a numeral 1 and 2, respectively

Table 1. Range of input variables in the database used to generalise the NN

an ascending order with respect to the shear span-to-depth ratio as one of the most influential parameters on shear strength of deep beams. In every four specimens, the first and the third deep beams were then chosen for training subset, and the second and fourth specimens were selected for validation and test subsets, respectively. The distribution of each parameter across its range in the training subset is manually examined to ensure that it covers the range of input parameters. If the range of input in the training subset fails to cover the entire distribution of the database, the rows in the database were rearranged until input of training subset could cover the entire distribution of the database range as shown in Table 1 and Fig. 3.

2.4. Building of neural network

The NN toolbox available in MATLAB Version 6.0⁴⁴ was used for building of the current NN model. Ashour and Alqedra²² showed that NN algorithms in MATLAB Version 6.0 can be conveniently implemented and used to model large-scale problems. In a multi-layered NN having a back-propagation algorithm, the combination of non-linear and linear transform functions can be trained to approximate any function arbitrarily well.⁴⁴ In the present NNs, tan-sigmoid transform function was employed in the hidden layers as it is generally known to be more suitable for multi-layer networks developed for non-linear applications than log-sig function that generates outputs between 0 and 1,⁴⁴ and linear transform function was adopted in the output layer. As upper and lower bounds of the tan-sigmoid function output are +1 and -1, respectively, input and target in database were normalised using equation (1) below so that they fall in the interval [-1, 1]. NNs can also have better efficiency with the normalisation of original data^{23,24}

$$1 \quad (p_i)_n = \frac{2(p_i - (p)_{\min})}{(p)_{\max} - (p)_{\min}} - 1$$

where $(p_i)_n$ and p_i are normalised and original values of data

set, and $(p)_{\min}$ and $(p)_{\max}$ represent minimum and maximum values of the parameter under normalisation, respectively. Also, after training and simulation, outputs having the same units as the original database can be obtained by rearranging equation (1) as follows

$$2 \quad p_i = \frac{[(p_i)_n + 1][(p)_{\max} - (p)_{\min}]}{2} + (p)_{\min}$$

Overfittings in training and outputs of NNs are commonly influenced by the number of hidden layers and neurons in each hidden layer. A trial and error approach was therefore carried out to choose an adequate number of hidden layers and number of neurons in each hidden layer as given in Table 2. In addition, NN performance is significantly dependent on initial conditions²³ such as initial weights and biases, back-propagation algorithms, and learning rate. In NNs presented in Table 2, the following features were applied

- initial weights and biases were randomly assigned by MATLAB version 6.0
- resilient back-propagation algorithm was used for back-propagation as a slower convergence is more effective in early stopping to generalise NN²⁴
- the learning rate and momentum factor were 0.4 and 0.2, respectively as proved to achieve more successful training of NN²¹
- mean square error (MSE) was used to monitor the network performance, where $MSE = \frac{1}{N} \sum_{i=1}^N (T_i - A_i)^2$, N is total number of training set, T_i and A_i are target and actual output of specimen i , respectively
- the maximum number of iterations (epochs) was 300.

In the training process of the multi-layer feed-forward NNs developed, the error between the prediction of the output layer and expected shear strength of deep beams was then back-propagated from the output layer to the input layer in which the connection weights and biases were modified. The training process was repeated until the maximum epochs was reached,

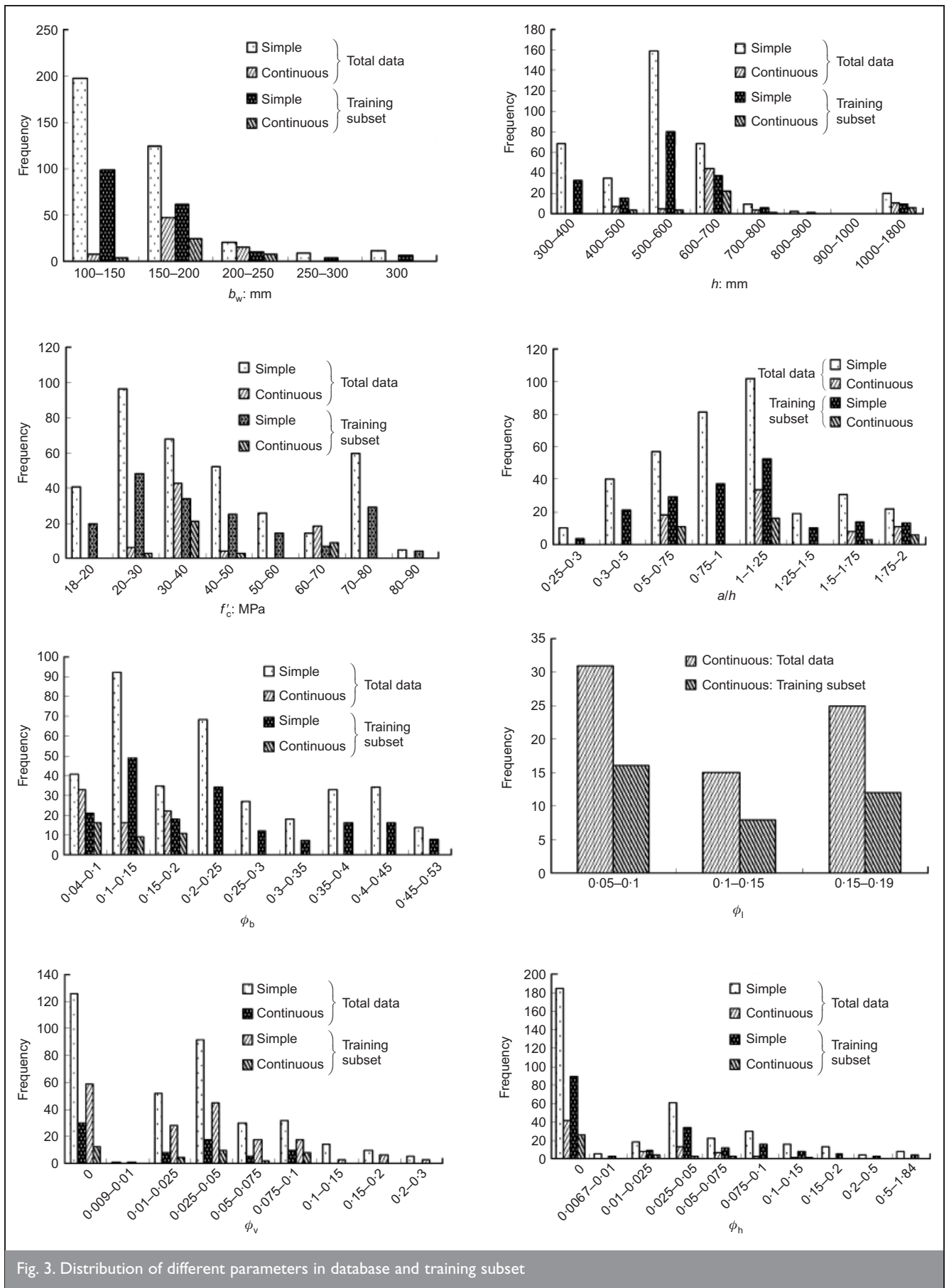


Fig. 3. Distribution of different parameters in database and training subset

the performance was minimised to the required target, MSE was less than 0.0001, the performance gradient falls below a minimum value, or the validation set error starts to rise for a number of iterations.

Statistical comparisons between outputs and targets for total points of database according to the number of hidden layers and the number of neurons in each hidden layer are given in Table 2. Each statistical value in Table 2 is an average

Network structures*	Mean ($\gamma_{cs,m}$)	Standard deviation ($\gamma_{cs,s}$)	Coefficient of determination (R^2)
$9 \times 9 \times 1$	1.020	0.210	0.910
$9 \times 18 \times 1$	1.010	0.193	0.937
$9 \times 27 \times 1$	1.019	0.205	0.925
$9 \times 18 \times 9 \times 1$	1.030	0.220	0.904
$9 \times 18 \times 9 \times 9 \times 1$	1.023	0.210	0.904

*The first and the last numbers indicate the numbers of neurons in input and output layers, respectively, and the others refer to the number of neurons in hidden layers.

Table 2. Comparison of outputs and targets according to different network structures

calculated from 30 different trials, as different random initial weights and biases are employed in each trial. Although the mean and standard deviation of the ratio of predicted and measured shear capacities of deep beams presented in Table 2 by different NN architectures were similar, the $9 \times 18 \times 1$ network is the most successful, achieving the closest predictions (the mean of the ratio between the prediction to experimental shear strengths is 1.01) and the least standard deviation of 0.193. In addition, overfitting seldom occurred in the $9 \times 18 \times 1$ network. The $9 \times 18 \times 1$ neural network shown in Fig. 1 with initial weights and biases therefore achieved the highest coefficient of determination of all 30 trials was finally selected for predicting shear strength of deep beams.

3. COMPARISONS WITH STRUT-AND-TIE MODELS

Several researchers^{10,12} showed that strut-and-tie models can be effectively used to predict shear strength of reinforced concrete deep beams. ACI 318-05¹ and Eurocode 2¹³ also recommend the use of strut-and-tie models for designing deep beams. Fig. 4 shows schematic strut-and-tie models of simple and continuous deep beams based on ACI 318-05 and Tan and Cheng.¹² Also, formulae suggested by ACI 318-05,¹ Siao,¹⁰ and Tan and Cheng¹² to predict shear strength of deep beams using strut-and-tie models are summarised in Table 3. These formulae showed that shear strength predicted by strut-and-tie models is greatly dependent on the width and inclination of compressive struts, the effective strength of concrete and amount of web reinforcement. No shear transfer mechanism of web reinforcement was specified in ACI 318-05, whereas shear transfer capacity of web reinforcement in the models by Siao and Tan and Cheng models is influenced by the inclination of struts. In addition, effectiveness factor of concrete in ACI 318-05 is 0.6 or 0.75, depending on the amount of web reinforcement and independent of concrete strength and shear span-to-overall depth ratio, whereas no effectiveness factor is used in the other two models as shear transfer capacity of concrete in Siao's model was determined from regression analysis of test results and Tan and Cheng's model used the modified Mohr–Coulomb failure criterion at the bottom nodal zone. Among the three models, size effect was only considered in Tan and Cheng's model, represented by the factor ψ as given in Table 3.

Table 4 gives the mean and standard deviation of the ratio between predicted and measured shear capacities, $\gamma_{cs} = (V_n)_{Pre.}/(V_n)_{Exp.}$, of simple and continuous deep beams

with different web reinforcement arrangement. Also, the distributions of γ_{cs} for all specimens in the database against shear span-to-overall depth ratio are shown in Fig. 5; Fig. 5(a) for strut-and-tie model of ACI 318-05, Fig. 5(b) for Siao's formula, Fig. 5(c) for Tan and Cheng's model and Fig. 5(d) for $9 \times 18 \times 1$ NN. For ACI 318-05's model, a better mean and standard deviation is shown in beams without or with orthogonal web reinforcement than those with only vertical or horizontal web reinforcement as given in Table 4. The largest standard deviation of all four models is demonstrated by Siao's formula. Predictions obtained from Tan and Cheng's model overestimate the shear strength of continuous deep beams with only horizontal web reinforcement; namely, the mean γ_{cs} for continuous deep beams with only horizontal web reinforcement is 1.121. For all three strut-and-tie models, predictions become highly unconservative with the increase of shear span-to-overall depth ratio and higher $\gamma_{cs,m}$ and $\gamma_{cs,s}$ are observed in continuous deep beams than in simple deep beams as shown in Table 4 and Fig. 5. On the other hand, predictions obtained from the $9 \times 18 \times 1$ NN are in better agreement with test results regardless of shear span-to-overall depth ratio and configuration of web reinforcement, even in continuous deep beams; $\gamma_{cs,m}$ and $\gamma_{cs,s}$ are 1.028 and 0.154, respectively, for simple deep beams, and 1.0 and 0.122, respectively, for continuous deep beams.

4. PARAMETRIC STUDY

The developed $9 \times 18 \times 1$ NN was utilised to examine the effect of different influencing parameters on shear strength of simple deep beams, namely, the effect of longitudinal bottom reinforcement, size effect, relative effectiveness of vertical and horizontal web reinforcement, and shear span-to-overall depth ratio on the shear strength of deep beams. The trend of continuous deep beam shear strength predicted by the developed NN for different parameters was not as smooth as that for simply supported deep beams as the test results in the database for continuous deep beams were relatively small; it is therefore not presented here. The trends predicted from this parametric study can also ensure that training and validation subsets in the developed NN were suitably built.

4.1. Effect of longitudinal reinforcement ratio

The influence of longitudinal bottom reinforcement index, $\phi_b = (\rho_s f_y / f'_c)$, on the normalised shear strength, $\lambda_n = V_n / (b_w h \sqrt{f'_c})$, of simple deep beams without web reinforcement for three different shear span-to-overall depth ratios is shown in Fig. 6. The normalised shear strength obtained from the NN increases with the increase of ϕ_b up to a certain limit beyond which λ_n remains constant. This limit of ϕ_b decreases with the decrease of shear span-to-overall depth ratio. This trend was experimentally observed by Tan *et al.*,⁴⁰ and analytically proved by Ashour.¹⁴

4.2. Relative effectiveness of vertical and horizontal web reinforcement

Figure 7 shows the variation of λ_n of simple deep beams with only vertical or horizontal web reinforcement against shear span-to-overall depth ratio. Vertical, ϕ_v , and horizontal, ϕ_h , web reinforcement indices are changed from 0.0 to 0.09 with interval of 0.03. Shear strength λ_n of deep beams decreases with the increase of shear span-to-overall depth ratio a/h up to a certain limit ($a/h=1.5$), beyond which the variation of λ_n

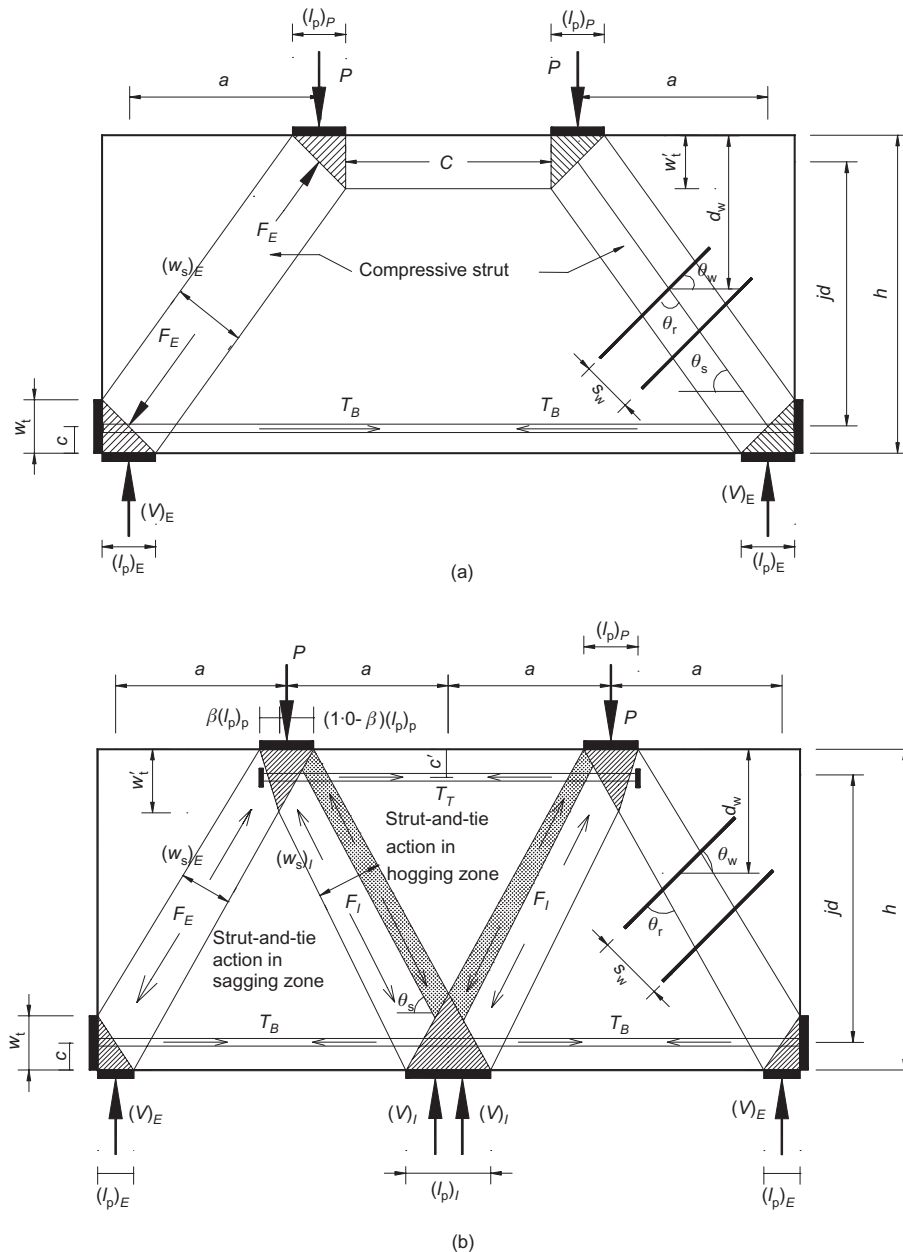


Fig. 4. Schematic strut-and-tie model for deep beams: (a) simply supported beams; (b) continuous beams. Definition of different parameters is given in Notation

would be negligible as observed by other experimental investigations.^{31,36} Also, the influence of vertical web reinforcement on the shear strength of deep beams is dependent on the shear span-to-overall depth ratio as pointed out by several researchers.^{3,4,36} The larger the shear span-to-overall depth ratio, the higher the influence of ϕ_v on the shear strength of deep beams; namely, when shear span-to-overall depth ratio is more than 0.75, shear strength of deep beams increases with the increase of ϕ_v , but that of deep beams having a smaller shear span-to-overall depth ratio is nearly independent of ϕ_v . On the other hand, the influence of ϕ_h on the shear strength enhancement of deep beams is independent of shear span-to-overall depth ratio. It is also observed that the critical shear span-to-overall depth ratio, where both vertical and horizontal web reinforcements are equally effective, is around 0.65, indicating that a higher shear strength exhibited by beams with only horizontal web reinforcement than beams

with only vertical web reinforcement when shear span-to-overall depth ratio is less than this critical threshold.

4.3. Effect of overall depth of deep beams

The influence of section overall depth, h , on the λ_n is presented in Fig. 8. It is clearly observed that the normalised shear strength of simple deep beams decreases with the increase of h , but no meaningful size effect appears in deep beams having h above 1000 mm. The decreasing rate of λ_n against the increase of h is more notable in beams having a smaller shear span-to-overall depth ratio a/h as the transverse tensile strain in concrete struts increases with the decrease of a/h . It is also pointed out by Tan and Cheng¹² that the smaller a/h , the higher the size effect as it is greatly influenced by strut action carrying very high compressive forces as predicted by the trained NN in Fig. 8.

Researcher	Shear capacity of deep beams (V_n)
ACI 318-05 ¹	$V_n = v_e f'_c b_w w_s \sin \theta_s;$ where $v_e = 0.75$ for beams having orthogonal web reinforcement ratio with $\sum \frac{A_{wj}}{b_w s_{wj}} \sin(\theta_r)_j \geq 0.003$ and otherwise 0.6; $\tan \theta_s = jd/a;$ $jd = h - c - w'_t/2$ for simple beams; $jd = h - c - c'$ for continuous beams; $w_s = \frac{2.25 w_t \cos \theta_s + [(l_p)_E + (l_p)_P] \sin \theta_s}{2}$ for simple beams; $w_s = \frac{(w_t + 2c') \cos \theta_s + [0.5(l_p)_l + (1 - \beta)(l_p)_p] \sin \theta_s}{2}$ for continuous beams.
Siao ¹⁰	$V_n = 1.05 \sqrt{f'_c} [1 + n(\rho_h \sin^2 \theta + \rho_v \cos^2 \theta)] b_w d$ where $\tan \theta = h/a$.
Tan and Cheng ¹²	$V_n = \frac{l}{(\sin 2\theta_s / f_t A_c) + (1/\psi f'_c A_{str} \sin \theta_s)}$ where $f_t = \frac{2A_s f_y \sin \theta_s}{A_c / \sin \theta_s} + \sum \frac{2A_w f_{yw} \sin(\theta_s + \theta_w) d_w}{A_c / \sin \theta_s} \frac{d_w}{d} + 0.5 \sqrt{f'_c};$ $\psi = \xi \cdot \zeta; \xi = 0.8 + \frac{0.4}{\sqrt{1 + (l_s - w_s)/50}};$ $\zeta = 0.5 + \sqrt{\frac{k d_s}{l_0}} \leq 1.2; k = \frac{\sqrt{\pi}}{2} \sqrt{\frac{f_y}{0.5 \sqrt{f'_c}}}$

Note : Definitions of different parameters used in the above formulas are given in the notation.

Table 3. Summary of shear strength prediction formulas using strut-and-tie model

Statistical values	Deep beam	Models	W/O	W/V	W/H	W/VH	Total
$\gamma_{cs,m}$	Simple	NN	1.042	1.007	1.045	1.044	1.028
		ACI 318-05 ¹	0.971	0.821	0.835	0.980	0.914
		Siao ¹⁰	1.460	1.169	1.318	1.228	1.274
		Tan and Cheng ¹²	0.925	0.864	0.902	0.852	0.878
	Continuous	NN	1.028	1.030	0.970	0.988	1.000
		ACI 318-05 ¹	1.244	0.817	1.118	0.984	1.000
$\gamma_{cs,s}$	Simple	Siao ¹⁰	1.813	1.555	1.926	1.496	1.675
		Tan and Cheng ¹²	1.034	0.813	1.121	0.843	0.931
		NN	0.193	0.155	0.136	0.142	0.154
		ACI 318-05 ¹	0.405	0.385	0.346	0.311	0.366
	Continuous	Siao ¹⁰	0.672	0.499	0.495	0.384	0.516
		Tan and Cheng ¹²	0.272	0.309	0.253	0.151	0.246
		NN	0.098	0.100	0.182	0.105	0.122
		ACI 318-05 ¹	0.399	0.216	0.422	0.207	0.348
		Siao ¹⁰	0.793	0.372	0.748	0.426	0.594
		Tan and Cheng ¹²	0.235	0.158	0.354	0.124	0.255

Note : $\gamma_{cs,m}$ and $\gamma_{cs,s}$ indicate the mean and standard deviation for the factor γ_{cs} , respectively.

W/O, W/V, W/H and W/VH refer to deep beams without, with only vertical, with only horizontal and with orthogonal web reinforcement, respectively

Table 4. Statistical comparisons of predictions by different methods

5. CONCLUSIONS

An optimum multi-layered feed-forward NN model, consisting of an input layer of nine neurons, a hidden layer of 18 neurons and an output layer of one neuron, was constructed to predict the shear strength of deep beams. The developed neural network employed a resilient back-propagation algorithm and

early stopping technique to improve generalisation of the NN. Training, validation and test subsets of the NN had 50%, 25%, and 25%, respectively, of the database with a total of 362 simple and 71 continuous deep beam specimens. Based on the statistical comparisons and parametric study, the following conclusions may be drawn.

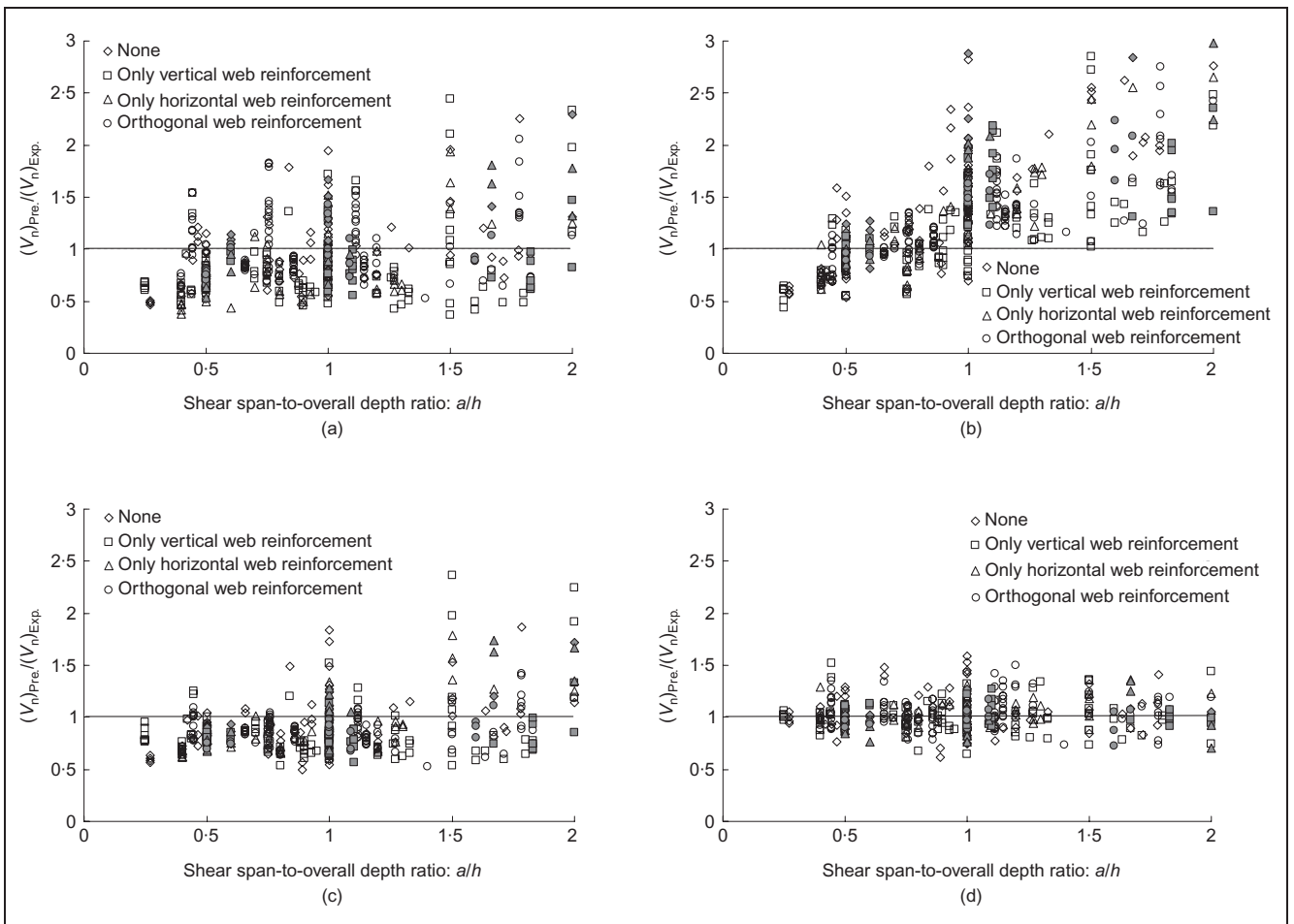


Fig. 5. Comparisons of predicted and measured shear strengths: (a) ACI 318-05;¹ (b) Siao;¹⁰ (c) Tang and Cheng;¹² (d) NN. White and black symbols indicate simple and continuous deep beams respectively

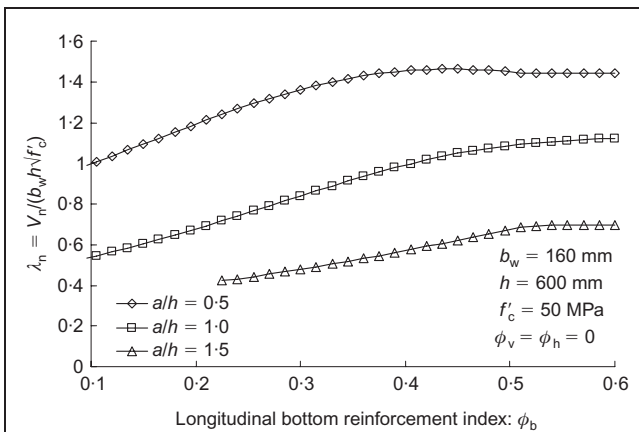


Fig. 6. Effect of ϕ_b on normalised shear strength of deep beams

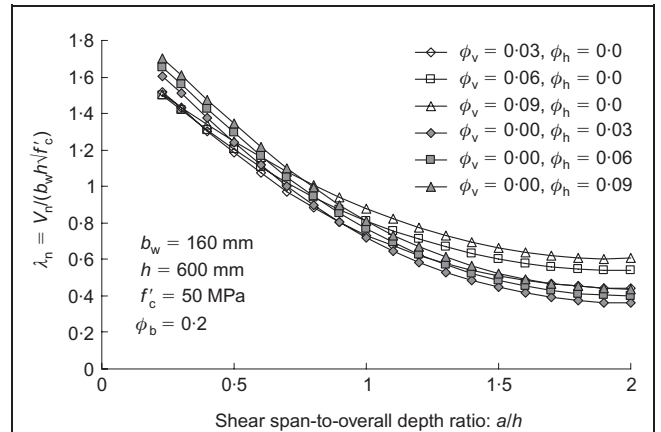


Fig. 7. Relative effectiveness of vertical and horizontal web reinforcement against a/h

(a) The predictions obtained from the NN are in much better agreement with test results than those determined from strut-and-tie models proposed by ACI 318-05,¹ Siao¹⁰ and Tan and Cheng.¹² The mean and standard deviation of the ratio between predicted using the NN and experimentally measured shear capacities are 1.028 and 0.154, respectively, for simple deep beams, and 1.0 and 0.122, respectively, for continuous deep beams. The developed

neural network should, however, be used for predicting shear strength of deep beams within the range of different parameters in the database.

(b) The normalised shear strength obtained from the NN increases with the increase of longitudinal bottom reinforcement index up to a certain limit beyond which it remains constant. The limiting point decreases with the decrease in shear span-to-overall depth ratio.

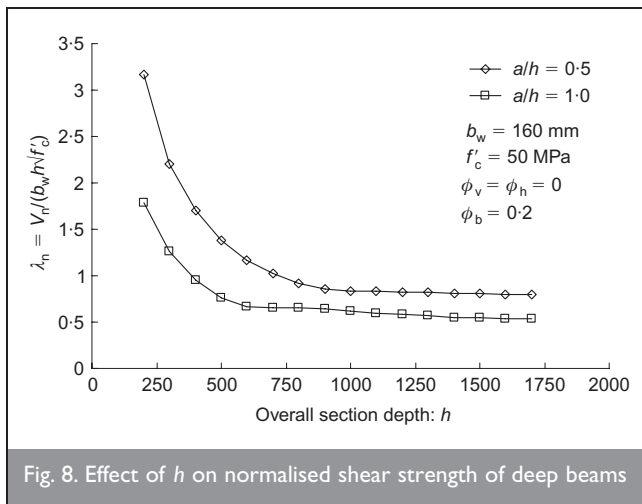


Fig. 8. Effect of h on normalised shear strength of deep beams

- (c) Shear strength of deep beams decreases with the increase of shear span-to-overall depth ratio up to shear span-to-overall depth ratio of 1.5, beyond which the variation of normalised shear strength would be negligible.
- (d) The critical shear span-to-overall depth ratio, where both vertical and horizontal web reinforcements are equally effective, is around 0.65; namely, a higher shear strength developed in beams with only horizontal web reinforcement than beams with only vertical web reinforcement when shear span-to-overall depth ratio is less than this critical threshold.
- (e) The normalised shear strength of deep beams decreases with the increase of overall section depth, but no meaningful size effect appears in deep beams having overall section depth above 1000 mm.

ACKNOWLEDGEMENTS

This work was supported by the Regional Research Centers Program (Bio-housing Research Institute), granted by the Korean Ministry of Education & Human Resources Development. The authors wish to express their gratitude for financial support.

REFERENCES

1. AMERICAN CONCRETE INSTITUTE (ACI). *Building Code Requirements for Structural Concrete (ACI 318-05) and Commentary (ACI 318R-05)*. ACI 318-05. ACI, Detroit, 2005.
2. ASHOUR A. F. Tests of reinforced concrete continuous deep beams. *ACI Structural Journal*, 1997, 94, No. 1, 3–12.
3. ROGOWSKY D. M., MACGREGOR J. G. and ONG S. Y. Tests of reinforced concrete deep beams. *ACI Structural Journal*, 1986, 83, No. 4, 614–623.
4. YANG K. H., CHUNG H. S. and ASHOUR A. F. Influence of shear reinforcement on reinforced concrete continuous deep beams. *ACI Structural Journal*, 2007, 104, No. 4, 420–429.
5. DE PAIVA H. A. R. and SIESS C. P. Strength and behavior of deep beams in shear. *Journal of Structural Engineering*, ASCE, 1965, 91(ST5), 19–41.
6. RAMAKRISHNAN V. and ANANTHANARAYANA Y. Ultimate strength of deep beams in shear. *ACI Journal*, 1968, 65, No. 2, 87–98.

7. KONG F. K., ROBINS P. J., SINGH A. and SHARP G. R. Shear analysis and design of reinforced concrete deep beams. *Structural Engineer*, 1972, 50, No. 10, 405–409.
8. CONSTRUCTION INDUSTRY RESEARCH AND INFORMATION ASSOCIATION (CIRIA). *Guide 2: The Design of Deep Beams in Reinforced Concrete*. Ove Arup and Partners, London, 1984.
9. AMERICAN CONCRETE INSTITUTE (ACI). *Building Code Requirements for Structural Concrete (ACI 318-99) and Commentary (ACI 318R-99)*. ACI 318-99. ACI, Detroit, 1999.
10. SIAO W. B. Strut-and-tie model for shear behavior in deep beams and pile caps failing in diagonal splitting. *ACI Structural Journal*, 1993, 90, No. 4, 356–363.
11. TJHIN T.N. and KUCHMA D. A. Alternative design for the non-slender beam (deep beam). In *Examples for the Design of Structural Concrete with Strut-and-Tie Models* (REINECK K. H. (ed.)). ACI International, Detroit, 1990, SP-208, pp. 81–90.
12. TAN K. H. and CHENG G. H. Size effect on shear strength of deep beams: investigating with strut-and-tie model. *Journal of Structural Engineering*, ASCE, 2006, 132, No. 5, 673–685.
13. BRITISH STANDARDS INSTITUTION. *European Standard EN 1992-1-1:2004. Eurocode 2: Design of Concrete Structures*. BSI, London, 2004.
14. ASHOUR A. F. Shear capacity of reinforced concrete deep beams. *Journal of Structural Engineering*, ASCE, 2000, 126, No. 9, 1045–1052.
15. WANG W., JIANG D. H. and HSU C. T. T. Shear strength of reinforced concrete deep beams. *Journal of Structural Engineering*, ASCE, 1993, 119, No. 8, 2294–2312.
16. ASIN M. *The Behaviour of Reinforced Concrete Continuous Deep Beams*. Delft University Press, Netherlands, 1999.
17. CHEUNG Y. K. and CHAN H. C. Finite element analysis. In *Reinforced Concrete Deep Beams* (KONG F. K. (ed.)). Blackie/van Nostrand Reinhold, London, 1990, pp. 204–237.
18. MARTI P. Basic tools of reinforced concrete beam design. *ACI Structural Journal*, 1985, 82, No. 1, 46–56.
19. ASHOUR A. F. and MORLEY C. T. Effectiveness factor of concrete in continuous deep beams. *Journal of Structural Engineering*, ASCE, 1996, 122, No. 2, 169–178.
20. GOH A. T. C. Prediction of ultimate shear strength of deep beams using neural networks. *ACI Structural Journal*, 1995, 92, No. 1, 28–32.
21. SANAD A. and SAKA M. P. Prediction of ultimate shear strength of reinforced-concrete deep beams using neural networks. *Journal of Structural Engineering*, ASCE, 2001, 127, No. 7, 818–828.
22. ASHOUR A. F. and ALQEDRA M. A. Concrete breakout strength of single anchors in tension using neural networks. *Advanced Engineering Software*, 2005, 36, 87–97.
23. HAGAN M. T., DEMUTH H. B. and BEALE M. H. *Neural Network Design*. PWS Publishing, Boston, MA, 1996.
24. RUMELHART D. E., HINTON G. E. and WILLIAMS R. J. Learning representations by back-propagation error. *Nature*, 1986, 323, 533–536.
25. SHI J. J. Clustering technique for evaluating and validating neural network performance. *Journal of Computation in Civil Engineering*, ASCE, 2002, 16, No. 2, 152–155.
26. YANG K. H., EUN H. C., CHUNG H. S. and LEE E.T. Shear characteristics of high-strength concrete deep beams

- without shear reinforcement. *Engineering Structures*, 2003, 25, No. 8, 1343–1352.
27. YANG K. H., CHUNG H. S. and ASHOUR A. F. Influence of section depth on the structural behavior of reinforced concrete continuous deep beams. *Magazine of Concrete Research*, 2007, 59, No. 8, 575–586.
 28. KANI G. N. J. How safe are our large reinforced concrete beams? *ACI Journal*, 1967, 64, No. 3, 128–141.
 29. KONG F. K., ROBINS P. J. and COLE D. F. Web reinforcement effects on deep beams. *ACI Journal*, 1970, 67, No. 12, 1010–1017.
 30. MANUEL R. F., SLIGHT B. W. and SUTER G. T. Deep beam behavior affected by length and shear span variations. *ACI Journal*, 1971, 68, No. 12, 954–958.
 31. SMITH K. H. and VANTSIOTIS A. S. Shear strength of deep beams. *ACI Journal*, 1982, 79, No. 3, 201–213.
 32. FURUUCHI H., KODAMA T. and KAKUTA Y. Shear reinforcement in reinforced concrete deep beams. *Journal of Japan Concrete Institute*, 1989, 11, No. 2, 333–338.
 33. HAYASHIKAWA T., SAITOH F. and KAKUTA Y. Strength of reinforced concrete deep beams with shear reinforcement. *Journal of Japan Concrete Institute*, 1990, 12, No. 2, 319–324.
 34. WALRAVEN J.C. and LEHWALTER N. Size effects in short beams loaded in shear. *ACI Structural Journal*, 1994, 91, No. 5, 585–593.
 35. SATO Y., UEDA T. and KAKUTA Y. Shear strength of deep beams with horizontal bars and stirrups. *Journal of Japan Concrete Institute*, 1995, 17, No. 2, 839–844.
 36. TAN K. H., KONG F. K., TENG S. and GUAN L. High-strength concrete deep beams with effective span and shear span variations. *ACI Structural Journal*, 1995, 92, No. 4, 395–405.
 37. TAN K. H., KONG F. K., TENG S. and WENG L.W. Effect of web reinforcement on high-strength concrete deep beams. *ACI Structural Journal*, 1997, 94, No. 5, 572–582.
 38. TAN K. H., KONG F. K. and WENG L. W. High-strength concrete deep beams subjected to combined top-and bottom-loading. *Structural Engineer*, 1997, 75, No. 11, 191–197.
 39. TAN K. H. and LU H. Y. Shear behavior of large reinforced concrete deep beams and code comparisons. *ACI Structural Journal*, 1999, 96, No. 5, 836–845.
 40. TAN K. H., TENG S., KONG F. K. and LU H. Y. Main tension steel in high strength concrete deep and short beams. *ACI Structural Journal*, 1997, 94, No. 6, 752–768.
 41. LEE J. S. and KIM S. S. An experimental study on the shear behavior of reinforced concrete deep beams subject to concentrated loads. *Journal of Korean Concrete Institute*, 1999, 11, No. 1, 191–200.
 42. OH J. K. and SHIN S. W. Shear strength of reinforced high-strength concrete deep beams. *ACI Structural Journal*, 2001, 98, No. 2, 164–173.
 43. TAN K. H. and TANG C. Y. Direct strut-and-tie model for prestressed deep beams. *Journal of Structural Engineering*, ASCE, 2004, 127, No. 9, 1076–1084.
 44. DEMUTH H. and BEALE M. *Neural Network Toolbox for User with MATLAB*. The Math Works, Inc., USA, 2002.
 45. JENKINS W. M. A truss analogy and neural network for reinforced concrete deep beam analysis. *Proceedings of the Institution of Civil Engineers, Structures and Buildings*, 2002, 152, No. 3, 259–267.
 46. JENKINS W. M. Neural network weight training by mutation. *Computers and Structures Journal*, 2006, 84, No. 31–32, 2107–2112.

What do you think?

To comment on this paper, please email up to 500 words to the editor at journals@ice.org.uk

Proceedings journals rely entirely on contributions sent in by civil engineers and related professionals, academics and students. Papers should be 2000–5000 words long, with adequate illustrations and references. Please visit www.thomastelford.com/journals for author guidelines and further details.